

Journal of Korean Institute of surface Engineering  
Vol. 29, No. 5, Oct., 1996

## LOW TEMPERATURE DIAMOND GROWTH USING MICROWAVE PLASMA CVD

**Yukihiro SAKAMOTO**

*Chiba Institute of Technology, 17-1, Tsudanuma 2-chome, Narashino, Chiba, Japan*

**Matsufumi TAKAYA**

*Chiba Institute of Technology, 17-1, Tsudanuma 2-chome, Narashino, Chiba, Japan*

**Kibatsu SHINOHARA**

*Nihon Koshuha, Co.,Ltd, 1119, Nakayama-cho, Midori-ku, Yokohama, Kanagawa, Japan*

### ABSTRACT

Diamond films were grown at lower temperatures (630–813K) on Si, Al (1100P), and Al-Si(8A, 8B, 8C) alloy substrates using improved microwave plasma CVD apparatus in a mixed methane and hydrogen plasma. Improved microwave plasma CVD apparatus equipped water cooled substrate holder and the substrates were set up lower position than bottom line of the applicator waveguide. When the methane concentration was high and growth was conducted at lower pressures the diamond films were synthesized. Moreover the deposits on the scratched substrates formed flat surfaces consisting of fine grains. XRD results, the deposits were identified to cubic diamond. An analysis using Raman spectroscopy, further confirmed that diamond films deposited on the Si substrates were high quality. The deposits on the Al substrates, in contrast, contained amorphous carbon. While the quality of the deposits on the Al-Si substrates were differed with the substrate alloys.

### INTRODUCTION

It has past about 10 years after reports of hot filament CVD<sup>1)</sup> and microwave plasma CVD<sup>2)</sup> from NIRIM, and a lot of diamond growth papers using various CVD methods<sup>3-6)</sup> were reported. In these papers, carbon source was used with hydrogen and reaction gas was decomposed with thermal or plasma energies. Then substrate temperatures were from 1073K to 1273K. Consequently the substrate tempera-

ture was so high and substrate materials which used in CVD were limited. If the substrate temperature was able to decrease, the used substrate materials can be selected widely and moreover application field of CVD diamond magnified. So low temperature diamond synthesis was tried using various CVD methods. In ECR plasma CVD<sup>7)</sup>, the apparatus was so complex and expensive. Also cost for diamond synthesis became higher. Moreover high magnetic field was used to this appa-

ratus, diamond synthesis on magnetic substrate was so difficult. Many trials for low temperature diamond growth using microwave plasma CVD were reported<sup>8-13</sup>). Deposition rate at lower substrate temperature was lower than that of higher substrate temperature and nucleation densities of diamond decreased in oxygen contained reaction gas system though quality of deposited diamond became better. And hot filament CVD was difficult to be stabilized growth condition and reappearancelly in low temperature diamond synthesis<sup>14</sup>).

The Si substrate used very often in the papers which used CVD for diamond growth at lower temperature. But the materials which have lower melting point can be used in low temperature diamond growth.

In this paper, diamond synthesis using improved microwave plasma CVD on the Si, Al, and Al-Si alloy substrates which have low melting point was investigated. Also effects of carbon concentration and growth pressure for low temperature diamond growth were discussed.

## EXPERIMENTAL PROCEDURE

Microwave plasma CVD apparatus (Nihon Koushuuha/MPT-1000) was used for diamond synthesis. Fig.1 shows schematic illustration of diamond synthesis apparatus by improved microwave plasma CVD. This apparatus equipped water-cooled substrate holder and the size of the substrate holder was 2 inches in diameter. Table 1 shows diamond synthesis conditions. Si, Al, and Al-Si alloys scratched with diamond powders were used as the substrates. Substrate temperature was

controlled by microwave output power and growth pressure. Then substrate temperature was measured by both thermocouple and optical pyrometer.

The deposits were estimated by SEM (JEOL/JXA-840) for observation, XRD (MAC Science/MXP3A) for crystallization. For analysis of the quality, Raman spectroscopy (SPEX/RAMALOG) was used.

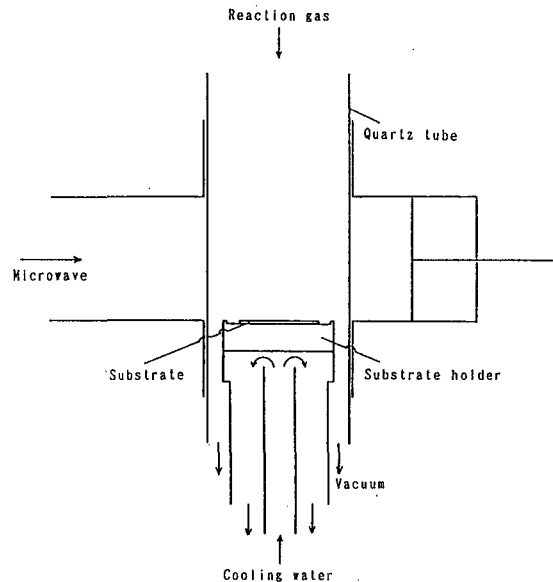


Fig. 1 Schematic illustration of diamond synthesis apparatus by improved microwave plasma CVD.

Table 1 Diamond synthesis conditions.

Total gas flowrate (SCCM)	200
Methane/hydrogen ratio (%)	1, 3, 5
MW power(W)	300~500
Pressure(kPa)	1.3, 4.0
Substrate temperature(K)	630~813
Reaction time (h)	7~25
Substrate <sup>0</sup>	Si, Al(1100P) Al-Si(8A, 8B, 8C)

## RESULT AND DISCUSSION

### Diamond synthesis on the Si substrates

Relationship between substrate temperatures and surface morphologies during diamond growth on the Si substrates was investigated. Fig. 2 shows the SEM image of the deposit on the Si substrate at 813K. Grain size of the diamond film was 0.5 to 1  $\mu\text{m}$  in diameter and well defined diamond crystals were observed. Fig. 3 shows the SEM image of the deposit at lower substrate temperature (668K). Fine diamond grains which have 0.2  $\mu\text{m}$  in diameter were observed. From the images of Fig. 2 and Fig. 3, grain size of the deposited diamond became smaller accompanied with decreasing of substrate temperature.

Fig. 4 shows the XRD pattern of the deposit at 668K. Diamond (111), (220), (311), and (400) peaks were observed and recognized to diamond. The deposits which synthesized from 643K to 813K showed same XRD patterns and also identified to diamond. More-

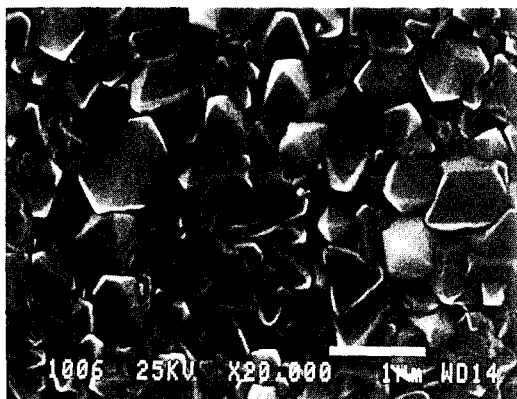


Fig. 2 SEM image of the deposit on the scratched Si substrate. (Methane/hydrogen; 6/194, pressure; 4.0 kPa, substrate temperature; 813K, reaction time; 7h)

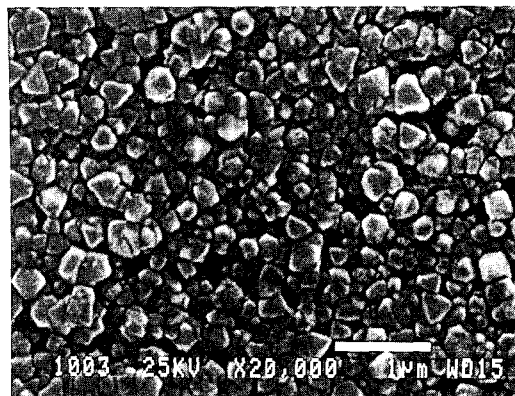


Fig. 3 SEM image of the deposit on the scratched Si substrate. (Methane/hydrogen; 6/194, pressure; 1.3 kPa, substrate temperature; 668K, reaction time; 7h)

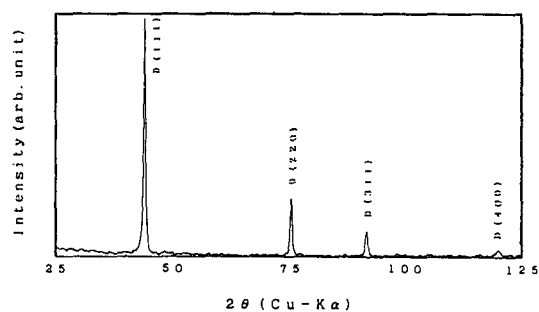


Fig. 4 XRD pattern of the deposit on the scratched Si substrate. (Methane/hydrogen; 6/194, pressure; 1.3 kPa, substrate temperature; 668K, reaction time; 7h)

over no graphite peak was observed from the deposits synthesized at low substrate temperature.

Furthermore qualities of the deposits were examined by Raman spectroscopy. Raman spectroscopy can detect non diamond elements such as graphite and amorphous carbon. Micro Raman measurement was used and diameter of laser light was about 1  $\mu\text{m}$  on the substrate. Fig. 5 shows the Raman spectrum of the deposit which showed in Fig.

2. Though grain size of the deposit was so small, but diamond peak was detected at  $1333\text{ cm}^{-1}$  and non diamond elements included little. Fig. 6 shows the Raman spectrum of the deposit which showed in Fig. 3. Also the diamond peak was detected at  $1333\text{ cm}^{-1}$  and inclusion of non diamond elements was so little. High quality diamond film can be obtained at lower substrate temperature by reducing of growth pressure and increasing of carbon source concentration.

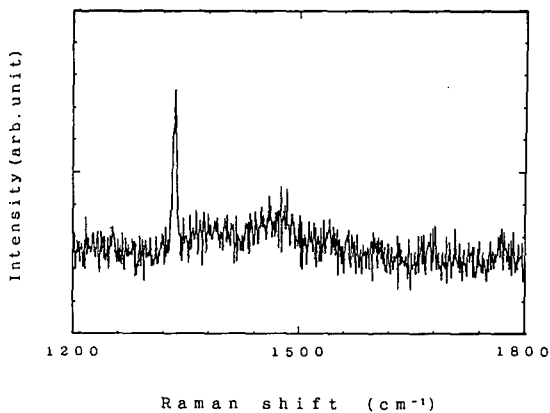


Fig. 5 Raman spectrum of the deposit on the scratched Si substrate.  
(Substrate temperature; 813K)

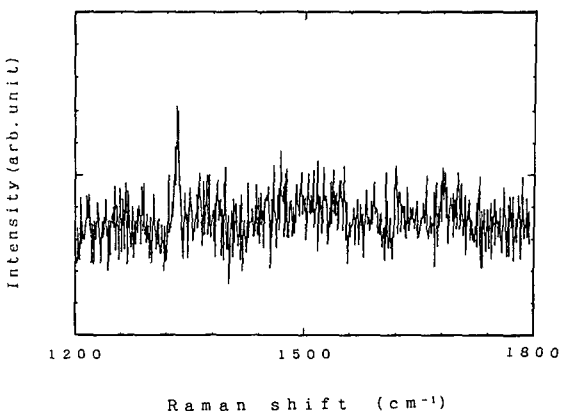


Fig. 6 Raman spectrum of the deposit on the scratched Si substrate.  
(Substrate temperature; 668K)

## Diamond synthesis on the Al and Al-Si alloy substrates

As diamond can be synthesized at lower substrate temperature on the Si substrate, so diamond synthesis on the Al (1100P) substrate which has low melting point and the Al-Si alloys (8A, 8B, 8C) which have good heat proof were studied.

SEM image of the deposit on the Al (1100P) substrate is showed in Fig. 7. Diamond film consisting of 0.1 to 0.5  $\mu\text{m}$  diamond particles was observed in the image.

Fig. 8 shows the XRD pattern of this sample. Al peaks, diamond (111), (220), (311), and graphite peaks were detected and the deposit identified to diamond film which contained graphite.

As graphite was detected in the XRD pattern, so Raman spectroscopy was used to analysis the quality of the deposits. Fig. 9 shows the Raman spectrum of the deposit which showed in Fig. 7. Though the broad amorphous carbon peaks at  $1350\text{ cm}^{-1}$ ,  $1500\text{ cm}^{-1}$ ,

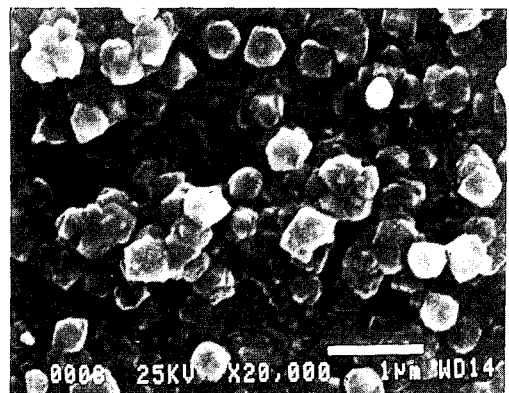


Fig. 7 SEM image of the deposit on the scratched Al (1100P) substrate.  
(Methane / hydrogen; 6 / 194, pressure; 1.3 kPa, substrate temperature; 640K, reaction time; 15h)

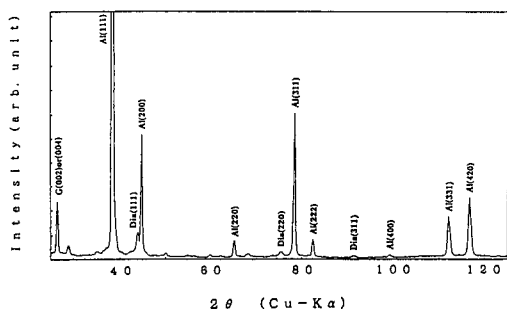


Fig. 8 XRD pattern of the deposit on the scratched Al (1100P) substrate.

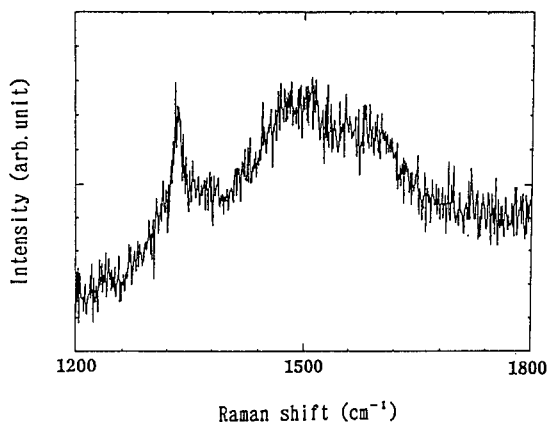
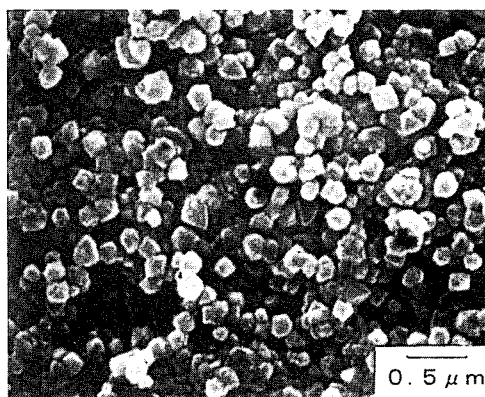


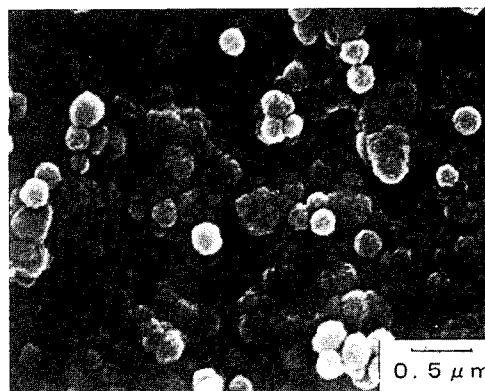
Fig. 9 Raman spectrum of the deposit on the scratched Al (1100P) substrate.

and the graphite peak at  $1580\text{ cm}^{-1}$  were detected, also diamond peak at  $1333\text{ cm}^{-1}$  detected remarkably.

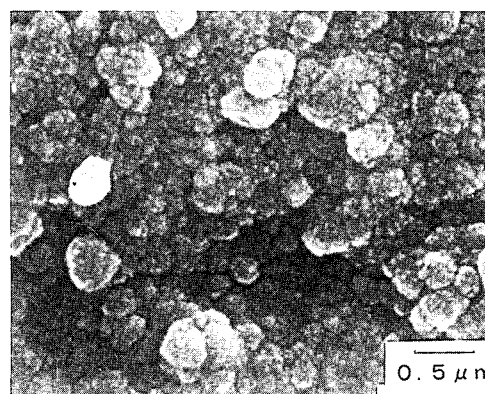
Fig. 10 shows the SEM images of the deposits on the Al-Si alloy substrates. The deposit on the Al-Si 8A alloy substrate (a) consisted of the grains whose size was about  $0.2\text{ }\mu\text{m}$  in diameter. The deposit on the Al-Si 8B alloy substrate (b) consisted of the spherical grains whose size is about  $0.2\text{ }\mu\text{m}$  in diameter and the film under the grains showed roundish morphology which contained non diamond elements. Also the deposit on the Al-Si 8C alloy substrate (c) showed more roundish morphology.



(a)



(b)



(c)

Fig. 10 SEM images of the deposits on the scratched Al-Si alloy substrates.  
 (a); 8A (substrate temperature;  $630\text{K}$ )  
 (b); 8B (substrate temperature;  $638\text{K}$ )  
 (c); 8C (substrate temperature;  $648\text{K}$ )

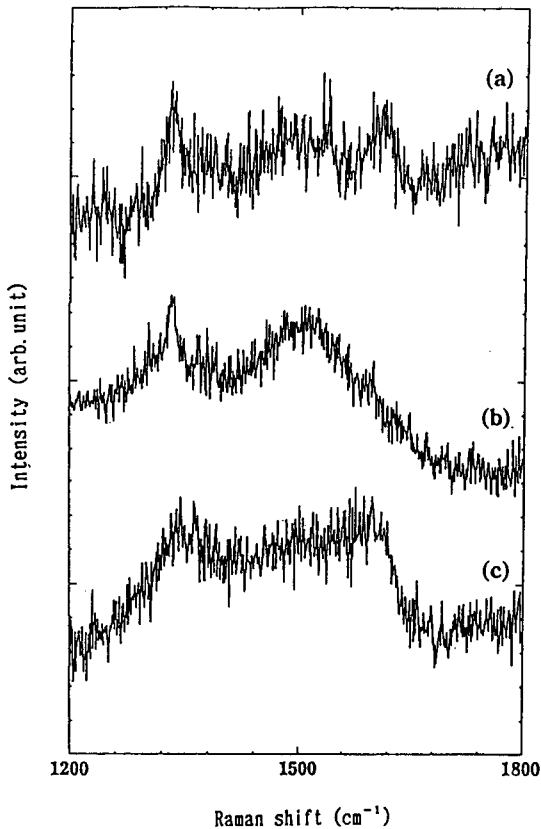


Fig. 11 Raman spectra of the deposits on the scratched Al-Si alloy substrates. (a);8A, (b);8B, and (c);8C

Raman spectroscopy was used to invest relationship between film qualities and surface morphologies. Fig. 11 shows Raman spectra of the deposits on the Al-Si alloy substrates. On the 8A substrate (a) diamond peak at  $1333\text{ cm}^{-1}$  and graphite peak at  $1580\text{ cm}^{-1}$  were detected. On the 8B substrate (b) intensity of the graphite peak decreased and amorphous carbon peaks at  $1350\text{ cm}^{-1}$  and  $1500\text{ cm}^{-1}$  become higher comparison with 8A. And on the 8C (c) these peaks on the 8B substrate and graphite peak at  $1580\text{ cm}^{-1}$  were detected. Though synthesis conditions were same, but the qualities of the deposits were

different.

From above, the qualities of the deposits, especially inclusion of non diamond elements were related to the chemical components of substrate materials.

### Discussion of the low temperature diamond growth mechanism

Diamond growth mechanism at lower substrate temperature was discussed.

Table 2 shows comparison of normal diamond synthesis plasma and lower substrate temperature diamond synthesis plasma. Accompanied with decreasing of the growth pressure, gas temperature ( $T_g$ ) fell, but electron temperature ( $T_e$ ) rose, so decomposition of methane increased. Moreover on the substrate, energy of the bombardment to the substrate became higher and activated species can be attached more to the substrate, because mean free path in the plasma became longer.

Combination of these reactions make possible to grow diamond at lower temperature by reducing of growth pressure and increasing of methane concentration.

Table 2 Comparison in normal diamond synthesis plasma (high pressure) and lower substrate

Factor	Kind of plasma	Normal plasma	Lower substrate temperature plasma
Plasma volume		Narrow	Wide
Pressure		High	Low
Carbon source concentration		Low	High
Mean free path		Short	Long
Sheath		Thin	Thick
Ne		Low	High
$T_e$		Low	High
$T_g$		High	Low

## CONCLUSIONS

Investigation results of low temperature diamond growth on the Si, Al, and Al-Si substrates using microwave plasma CVD are follows,

1) Low temperature diamond growth can be achieved by reducing of growth pressure and increasing of methane concentration.

2) The deposited films were flat and consisted of fine diamond grains.

3) The quality of the deposit on the Si substrate was not become worse in spite of low temperature growth.

4) The deposit on the Al substrate included more impurities than that of on the Si substrate.

5) The qualities of the deposits on the Al-Si alloy substrates differed with the substrate alloy material and related to chemical component of substrate materials.

## REFERENCES

1. S. Matsumoto, Y. Sato, M. Tsitsumi and N. Setaka; *J. of Mater. Sci.*, **17**, 3106 (1982)
2. M. Kamo, Y. Sato, S. Matsumoto, and N. Seataka; *J. of Cryst. Growth*, **62**, 642 (1983)
3. S. Matsumoto ; *J. of Mater. Sci. Lett.*, **4**, 600 (1985)
4. H. Kawarada, K. S. Mar and A. Hiraki ; *Jpn. J. of Appl. Phys.*, **26**, 6, L1032 (1987)
5. A. Sawabe and T. Inuzuka ; *Appl. Phys. Lett.*, **46**, 2, 146 (1985)
6. K. Suzuki, A. Sawabe, H. Yasuda and T. Inuzuka; *Appl. Phys. Lett.*, **50**, 23, 728 (1987)
7. C. R. Eddy, Jr., B. D. Sartwell and D. L. Youchison; *Surf. Coat. and Tech.*, **48**, 69 (1991)
8. Y. Liou, A. Inspektor, R. Weimer, and R. Messier; *Appl. Phys. Lett.*, **55**, 7, 631 (1989)
9. T. P. Ong and P. H. Chang; *Appl. Phys. Lett.*, **55**, 20, 2064 (1989)
10. W. L. Hsu, D. M. Tung, E. A. Fuchs, K. F. McCarty, A. Joshi, and R. Nimmagadda; *Appl. Phys. Lett.*, **55**, 26, 2740 (1989)
11. Y. Liou, R. Weimer, D. Knight, and R. Messier; *Appl. Phys. Lett.*, **56**, 5, 437 (1990)
12. Y. Muranaka, H. Yamashita, and H. Miyadera; *Surf. Coat. and Tech.*, **47**, 1 (1991)
13. Y. Muranaka, H. Yamashita, and H. Miyadera; *J. Appl. Phys.*, **69**, 12, 8145 (1991)
14. M. Ihara, H. Maeno, K. Miyamoto, and H. Komiyama; *Appl. Phys. Lett.*, **59**, 1473 (1991)